# Effects of Lignin on the Thermal and Morphological Properties and Damages Mechanisms after UV Irradiation of Polypropylene Biocomposites Reinforced with Flax and Pine Fibres: Acoustic Emission Analysis

Zouheyr Belouadah , Khaled Nasri , Lotfi Toubal *

Posted Date: 20 March 2024

doi: 10.20944/preprints202403.1242.v1

Keywords: biocomposites; UV aging; acoustic emission; damage mechanisms; environmental degradation; thermogravimetric analysis

*Article*

# Effects of Lignin on the Thermal and Morphological Properties and Damages Mechanisms after UV Irradiation of Polypropylene Biocomposites Reinforced with Flax and Pine Fibres: Acoustic Emission Analysis

**Zouheyr Belouadah [1], Khaled Nasri [2] and Lotfi Toubal [2,*]**

[1] Laboratoire des Sciences et Techniques de l'Environnement, Ecole Nationale Polytechnique, 10 Avenue des Freres Oudek, BP 182, El-Harrach, 16200 Alger, Algeria

[2] Innovations Institute in Ecomaterials, Ecoproducts and Ecoenergy (I2E3), Mechanical Engineering Department, Université du Quebec à Trois-Rivières, 3351 boul. des Forges, Trois Rivières, G9A 5H7, Canada

* Correspondence: lotfi.toubal@uqtr.ca

**Abstract:** Various wood fibres, including pine and flax, are used in wood–plastic composites (WPCs). This paper studies the effect of the lignin content on the morphological and thermal degradation and damage due to the ultraviolet (UV) aging of polypropylene/flax (PP-flax) and polypropylene/pine (PP-pine) fibres composites. Flax and pine fibres exhibited distinct densities of 1.51 and 1.47 g/cm$^3$, respectively, potentially influenced by growth factors and varying compositions of light substances, such as hemicellulose, lignin, and impurities. The thermal decomposition mass loss increased proportionally with the percentage of lignin in the fibre. From 238°C to 390°C, the pine fibre exhibited a 72% mass loss compared to flax fibre, which showed a 54% mass loss, owing to the higher lignin content in pine fibres. Based on differential scanning calorimetry (DSC), the fibre composition affected the material melting temperature. Moreover, DSC curves revealed a higher degree of crystallinity in the case of the PP-flax biocomposite (12%) compared to pure polypropylene (9%) and PP-pine (6%). This result can be attributed to the high content of crystalline components in flax fibres, such as cellulose. Acoustic emissions analysis confirmed that the high lignin content delays degradation and mitigates the appearance of microcracks on the surface of the PP-pine biocomposite. Overall, the study provides valuable data for understanding the UV degradation phenomenon in biocomposites and highlights the influence of fibre composition on material performance.

**Keywords:** biocomposites; UV aging; acoustic emission; damage mechanisms; environmental degradation; thermogravimetric analysis

## 1. Introduction

The integration of environmentally friendly materials in product design has contributed to the growth of the natural fibres and biocomposites market, with revenues expected to exceed USD 61.04 billion by 2030 [1]. The high-reinforcing capability of these fibres and their small environmental footprint compared to those of synthetic fibres have led to their increasing use in various industrial sectors, such as the automotive and construction sectors. For instance, in the construction sector, particularly in North America, biocomposites, also known as wood-plastic composites (WPCs) or natural fibre composites (NFCs), are widely used in the manufacturing of door and window frames, solid and hollow boards, and laminated flooring [2]. However, structures exposed to the outdoors

 doi:10.20944/preprints202403.1242.v1



undergo both ultraviolet (UV)- and moisture-induced damage, negatively affecting their mechanical properties.

The natural aging process, driven by unpredictable variations in temperature, humidity, and other environmental factors, leads to complex and unpredictable material degradation. In contrast, environmental chamber testing exposes materials to controlled, elevated temperatures, light intensities beyond those typically encountered outdoors, and shorter wavelengths of light. While accelerated aging tests do not replicate natural aging perfectly, they offer the significant advantage of simulating the aging of biocomposites in just a few weeks, a process that typically occurs outdoors over months or even years.

Biocomposites with short fibres are typically crafted from conventional thermoplastics, like polypropylene (PP) and polyethylene, amalgamated with short natural fibres spanning lengths from 0.1 to 2 mm. The degradation of these composites in the environment hinges on the type of natural fibres and the matrix. The hydrophilic nature of these fibres, coupled with their limited UV resistance, instigates fibre–matrix decohesion, consequently impeding the transfer of interfacial stresses [3–9]. This investigation focuses on flax and pine fibres. Flax boasts a substantial cellulose content, whereas pine fibres showcase distinct morphological features, unlike flax fibres, which are characterized notably by a high lignin content (28% contrasted with ~3% for flax [10,11]). Cellulose and hemicellulose modulate the yield strength and rigidity of biocomposites, while the hydrophobic nature of lignin acts as a binding agent for other components within natural fibres [10–13].

One can measure the initial properties of biocomposites, but predicting their evolution over time remains challenging. Exposure of biocomposites to UV radiation breaks covalent bonds, resulting in discoloration, yellowing, surface roughness, weight loss, deterioration of mechanical properties, and cracks [8–11,14]. For fibres, the aging process begins when UV radiation is absorbed by the lignin structure, forming chromophore groups, such as carboxylic acids, quinones, and hydroperoxyl radicals, responsible for yellowing and discoloration [14]. The photodegradation of polymers induces surface oxidation, chain scission, and, consequently, the breaking of bonding molecules. This process of degradation in polymer matrices leads to the formation of superficial cracks, significantly decreasing the tensile strength of biocomposites. Comprehensive literature reviews on the degradation mechanisms of biocomposites under UV exposure were presented in [7,10,11].

In this study, biocomposites were manufactured from granules of polypropylene biocomposite reinforced with 30% short flax fibres (PP30-F) or with 30% short pine fibres (PP30-P), obtained from Rhetech, Inc. (Whitmore Lake, MI, USA). Because of the absence of detailed characteristics regarding the constituents of composite granules, particularly natural fibres, and our belief that understanding the individual properties of these components is essential for analyzing final product behaviour, we performed the separation of the matrix (PP) from the natural fibres (flax and pine). This allowed us to assess and, more importantly, compare the performance of the studied materials on the scale of fibres and the composite, examining mechanical, physical, morphological, and thermal properties. Furthermore, during tensile tests, we utilized acoustic emission (AE) testing to study the progression of various damage mechanisms that ultimately lead to specimen failure. This technique offers advantages in terms of sensitivity to different types of damage in composites [15]. We select AE parameters, such as amplitude, duration, and energy, as evaluation indices and then correlate them with the material's mechanical behaviour. Thus, damages related to UV/humidity aging can be documented, and the influence of the chemical and morphological properties of these fibres on the damage threshold is better assessed. Ultimately, this study highlights the response of both types of fibres to the effects of UV degradation in these biocomposites.

This article is organized as follows. First, we describe the methodology, specimens, and measurement techniques in Section 2. Next, Section 3 presents the results and discussion, covering morphological analysis, thermal degradation, UV aging, and acoustic signatures of the fracture mechanisms in both composites. Finally, the main conclusions are drawn in Section 4.

## 2. Experiments

### *2.1. Materials, Specimens, and Tensile Testing*

 doi:10.20944/preprints202403.1242.v1



We used composite pellets of PP reinforced with 30% short flax fibres (PP-flax) or 30% short pine fibres (PP-pine), shown in Figure 1, to shape the tensile specimens. Considering the direct impact of the plant fibre chemical composition on the UV effect on composite durability and for better identification of the composite damage mechanisms, we identified the pellet composition by separating the different components and subsequently analyzing each constituent individually. The process of fibre–matrix separation is illustrated in Figure 2.

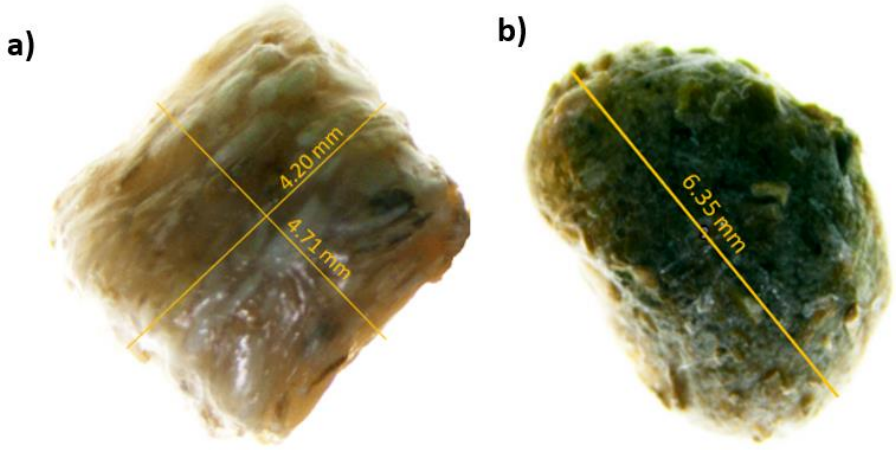


**Figure 1.** Composite pellets of PP reinforced with a) 30% short pine fibres and b) 30% short flax fibres.

Approximately 20 g of composite pellets were placed in an Erlenmeyer flask containing 150 mL of xylene solution. The mixture was stirred at 1500 rpm and heated to ~140°C until the pellets dissolved completely. We separated the fibres from the matrix using a sieve. This process was repeated several times until the complete removal of PP from the surface of the fibres.

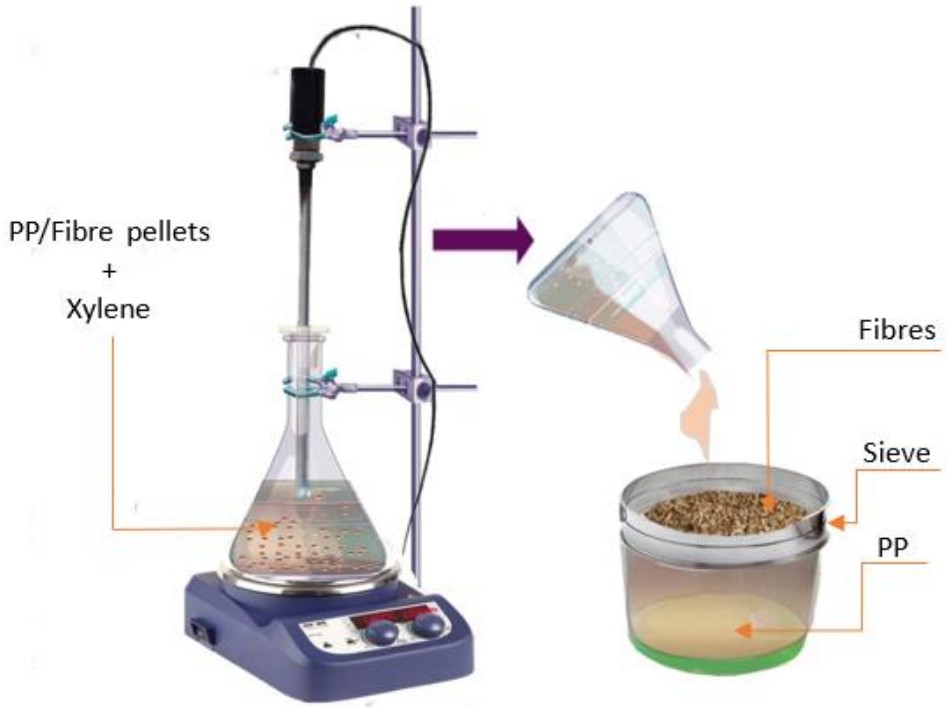


**Figure 2.** Fibre–matrix separation process.

 doi:10.20944/preprints202403.1242.v1



Utilizing the 100-TON HAITIAN ZHAFIR ZTR 900 press (Zhafir Zeres series ZE900/210, Haitian, Inc.), we performed injection moulding specifically for the production of tensile samples, per ASTM D-638 [16]. To mitigate the occurrence of micro-voids and porosity in the samples post-injection, the biocomposite granules underwent a pre-injection drying phase at 80°C for 2 h. The injection process was conducted at 200°C.

### *2.2. Characterization Methods*

#### 2.2.1. True Density Measurement

To determine the true density of composite pellets and their constituents, we employed a gas pycnometer. Around 3 g of a powder sample was analyzed ten times using Micromeritics AccuPyc II 1340 at 24°C under helium gas (He).

#### 2.2.2. Thermal Assessment

The temperature profiles for the thermogravimetric analysis (TGA) and DSC were determined from ambient conditions to 600°C in a nitrogen environment with a heating rate of 10°C/min using TA Instrument apparatus.

#### 2.2.3. ATR–FTIR Analysis

The chemical composition of the PP-pine and PP-flax composite pellets and their constituents PP, flax fibres, and pine fibres were examined using the attenuated total reflectance–Fourier transform infrared spectroscopy (ATR–FTIR) technique. This method is a robust tool for qualitative analysis. ATR–FTIR measurements were conducted with the IRTracer-100_NIS-PC-Instrument (SHIMADZU) at room temperature for wavenumbers ranging from 4000 to 400 $cm^{-1}$ and a spectral resolution of 4 $cm^{-1}$.

#### 2.2.4. Morphological Analysis

The aspect ratio of the fibres, representing the relationship between the length $L$ and diameter $D$ of the fibres incorporated in the composite pellets ($L/D$), was evaluated to assess this essential parameter that influences the mechanical and physical properties of the final material. For this evaluation, we examined the morphology of the short fibres thoroughly using an optical microscope. The samples were prepared appropriately and observed at various levels of magnification. This morphological analysis allowed for a detailed view of the fibre characteristics, including their size, shape, and uniformity.

### *2.3. Artificial Weathering*

The industry demands faster-accelerated weathering test results while maintaining a strong correlation with real-time exposure outcomes in laboratory simulations. Here, the aging conditions were conducted per ASTM G154-23 [17], standard practice for artificial UV aging of non-metallic materials. We know that the PP matrix degrades under the influence of UV rays, justifying the choice of the PP matrix as a reference for the study of biocomposites for comparison. However, the effect of UV aging on virgin PP has not been examined for two reasons. First, we could not access the PP used by Rhetech to manufacture the pellets used in this work. Second, pure PP exhibits high toughness [6], and our main objective in this research project was to analyze the impact of UV rays on the performance of biocomposites, with a particular focus on the influence of the chemical composition of natural fibres on their degradation. Exposure times in most weathering cycles, except for the dew cycle and fluorescent UV-condensation type (ASTM G53) exposure, range from 1000 to 2000 h. We conducted tests with exposures of up to 1400 hours, adhering to the standard practices outlined in the literature. Two environmental conditions were considered in this study:

1. UV without humidity. The samples were subjected to UV aging using UVA-340 fluorescent lamps (irradiance at a wavelength of 340 nm) in a QUV/SE aging apparatus (Q-Lab Co., USA).

 doi:10.20944/preprints202403.1242.v1



Aging lasted for two months, with 8 h of UV exposure at an irradiance of 1.55 W/m² at 60°C per day.

2. UV with humidity. The samples were the same as in Condition 1 for two months, but with 4 h of water condensation at 50°C after each UV exposure at 60°C.

### *2.4. Acoustic Emission*

AE measurements were conducted using two resonant MICRO-80 sensors operating within a 100–1000 kHz frequency range using a system provided by the Physical Acoustics Corporation (MISTRAS, USA). Before each test, three pencil lead break tests were conducted to calibrate the source location of AE events and assess the coupling state between the specimen and the sensors. We analyzed the recorded AE acoustic signals analyzed, considering parameters such as amplitude, count, duration, and frequency, as referenced in [6,13,15]. Utilizing the K-means clustering algorithm, we assigned each set of acoustic events to a specific damage mechanism.

## 3. Results and Discussion

### *3.1. Morphological Analysis*

The length-to-diameter ratio (*L*/*D*) plays a pivotal role in the mechanical properties of composite materials based on both flax and pine fibres. An optimal *L*/*D* enhances the load transfer among components, thus reinforcing their mechanical attributes. Inadequate values can give rise to weak points, jeopardizing the overall material strength. A precise balance of *L*/*D* proves essential to optimizing the mechanical performance of composites. Figure 3 exhibits microscopic images of the fibres. According to these images, we recorded *L*/*D* values of 4.82 and 3.17 for flax and pine fibres, respectively.

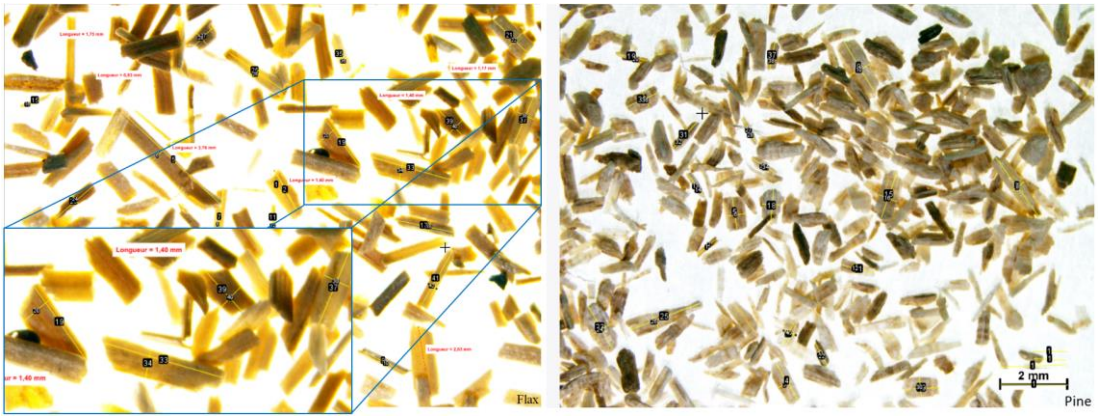


**Figure 3.** Microscopic micrographs of flax and pine fibres after separation from the matrix.

### *3.2. True Density Measurement*

The results of density and porosity analysis for various materials provide significant insights into their physical characteristics and potential performance (Figure 4). Plant fibres, despite their similar categorization, exhibit distinct densities of 1.51 and 1.47 g/cm³ for flax and pine fibre, respectively, potentially influenced by growth factors and varying compositions of light substances, such as hemicellulose, lignin, and impurities. PP, with a lower density of 0.98 g/cm³, stands out prominently and falls within the typical range of plastic densities.

Reinforced pellets reveal noteworthy disparities: the composite pellets PP-flax at 0.96 g/cm³ suggests post-fabrication porosities and a higher *L*/*D* for fibres, while the composite pellets PP-pine reaches 1.01g/cm³, possibly due to better fibre integration and for the lower *L*/*D* for fibres. Porosity, which is higher for plant fibres (34% for flax and 32% for pine), differs in composites (3% for flax and

 doi:10.20944/preprints202403.1242.v1



1.5% for pine). These results underscore the intricate impact of porosity and fibre–matrix interaction on composite properties, paving the way for in-depth research and targeted applications.

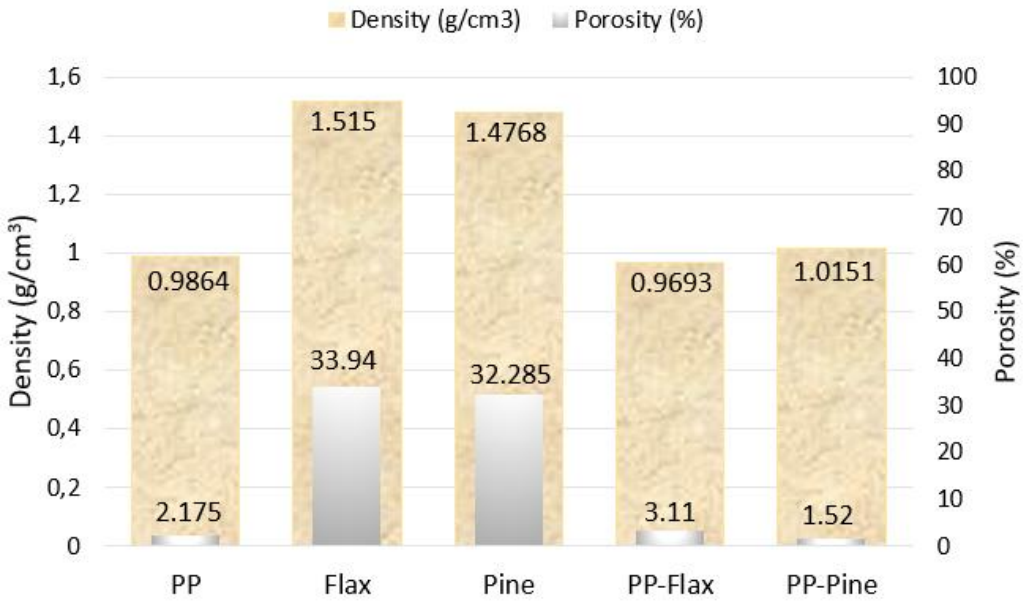


**Figure 4.** Comparison of density and porosity for composite pellets and their constituents.

*3.4. Thermogravimetric Analysis*

Thermal stability holds significance for natural fibres considered as potential reinforcements in composite materials. Manufacturing such materials often involves treatments at elevated temperatures, especially when the composite matrix is a thermoplastic. The thermal behaviour of composites is significantly influenced by the chemical composition of the fibres.

Figure 5a and b depict the thermogravimetric (TG) curve and its first derivative, respectively, for the composite pellets and their constituents. From these curves, three stages of thermal change become discernible as the temperature rises. The first stage is specifically associated with flax and pine fibres. Up to 100°C, decreases in mass by 5.57% and 7% for pine and flax fibres, respectively, are due to moisture loss, as reported in some works [18,19]. Subsequently, both fibre types maintain thermal stability until reaching 238°C for flax fibre and 247°C for pine fibre. This differentiation stems from the higher lignin content in pine fibres, thus retarding the thermal degradation of plant fibres. Manral et al. [15] highlighted that cellulose and hemicellulose degrade because of heat faster than lignin. Char formation during the thermal degradation of natural fibre is linked to lignin, which acts as an insulated layer for subsequent lignocellulosic fibre degradation. Higher lignin content enhances natural fibre's thermal stability.

The second stage relates only to fibres and composite pellets and occurs at 238°C to 390°C for flax and pine fibre and 260°C to 378°C for PP-flax and PP-pine. This phase sees significant decomposition of the fibre's main components. In the case of pine fibre, a 72% mass loss indicates a delay in decomposition compared to flax fibre, which experiences a 54% mass loss, owing to the higher lignin content in pine fibres. Burhenne et al. [20] observed that the TG curve of spruce wood with bark shifts approximately 20°k higher than the TG curves of straw and rape straw. This implies that breaking down woody biomass demands increased activation energy because of its elevated lignin content and distinct type when contrasted with straw. The same observation was reported by Kristanto et al. [21]. Of note, the thermal behaviour of fibres also impacts that of composite pellets. Slower thermal degradation is observed for PP-pine pellets, resulting in a 28% mass loss, while PP-flax pellets lose 13% mass. A recent study indicated an enhancement in the thermal stability of PAM and CMX hydrogels following the introduction of lignin [22]. For the third stage (up to 600°C), additional losses of 12% for flax fibre and 8% for pine fibre are noted.

 doi:10.20944/preprints202403.1242.v1



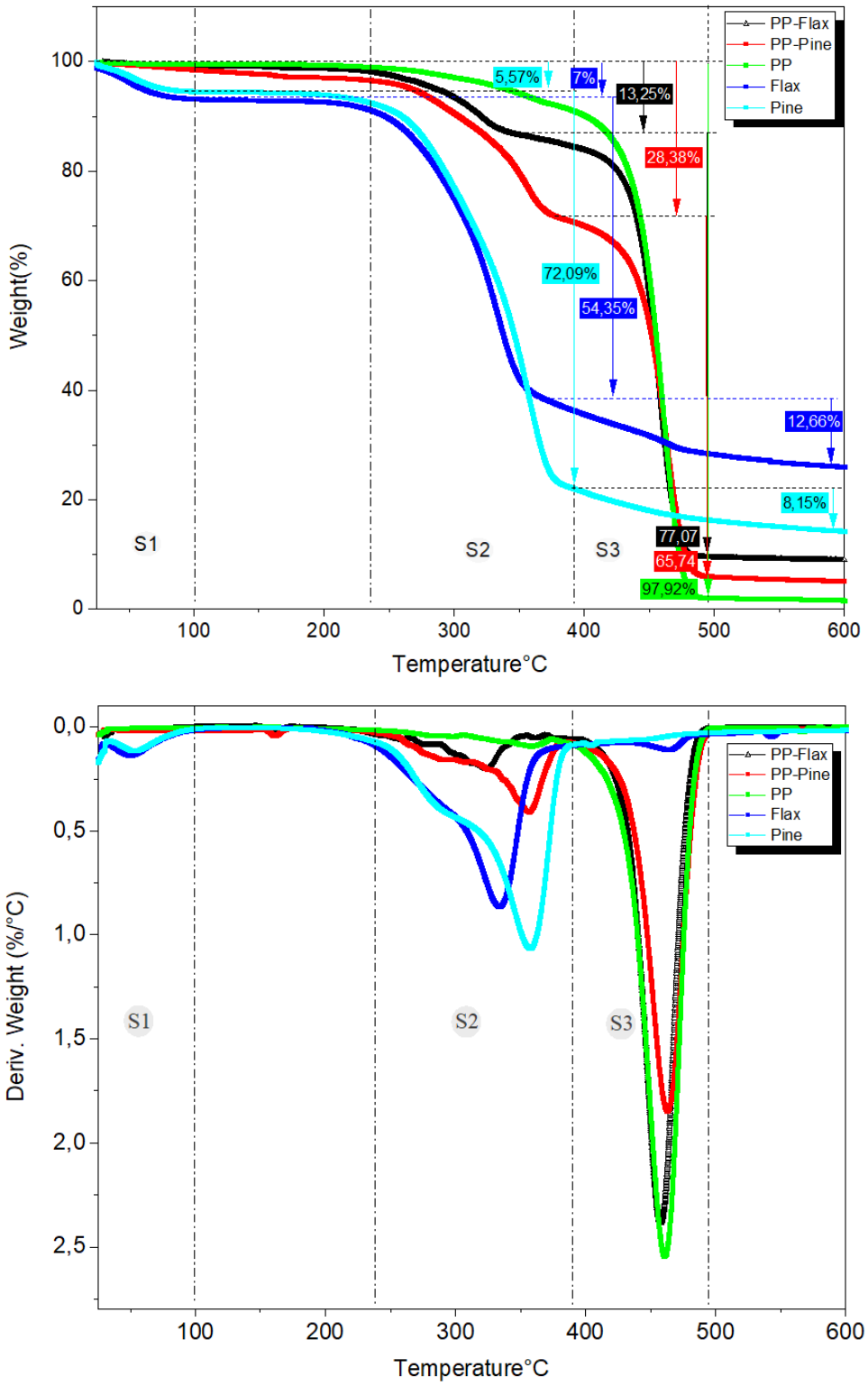


**Figure 5.** Thermogravimetric curves and first derivatives for composite pellets and their constituents.

*3.5. Differential Scanning Calorimetry Analysis*

Figure 5 shows the DSC curves, and the analysis results are presented in Table 1, alongside other previously published findings. An endothermic peak, observed at temperatures below 105°C for all five samples, is attributed to the evaporation of water present in natural fibres and PP. This peak aligns with the corresponding peak observed on the TG curves. The calculated enthalpy of water

 doi:10.20944/preprints202403.1242.v1



evaporation is 576 J/g for pine fibre, 466 J/g for flax fibre, 486 J/g for PP, 433 J/g for PP-pine, and 426 J/g for PP-flax. The enthalpy at this peak is directly proportional to the water content of the samples, which tends to be higher for natural fibres compared to samples containing PP (pure PP, PP-pine, PP-flax). The water content of natural fibres varies depending on the type of fibre, processing, storage conditions, and humidity levels. The three samples containing PP exhibited a peak at 162–163 °C, corresponding to the melting point of the PP. The calculated enthalpy around this peak is 18 J/g for PP, 12 J/g for PP-pine, and 26 J/g for PP-flax. The enthalpy of this peak is directly proportional to the fraction of crystallinity of the material, a value calculated using the following equation:

$$F_c = \Delta H_m / [\Delta H_m^0 (1 - x)] \quad (1)$$

where $F_c$ is the crystal fraction, $\Delta H_m$ is the enthalpy of fusion measured at the peak melting temperature of PP, and $\Delta H_m^0$ signifies the enthalpy of fusion of the crystal phase of PP at 100% crystallinity. The latter was determined using the value from [23], specifically 209 J/g.

The degree of crystallinity of PP depends on factors such as cooling rate, the degree of branching, molecular orientation, and the presence of additives or fillers [24]. In this study, it was higher for PP-flax (12%) than for pure PP (9%) and PP-pine (6%). The increase in crystallinity for flax fibre–reinforced pellets resulted from the positive effect of nucleation of flax fibre and the high content of crystalline components in flax fibres, such as cellulose [25,26]. In contrast, the decrease in crystallinity in the case of PP-pine was due to the dilution effect of pine fibre [27] and the presence of a high percentage of amorphous components, such as lignin.

Malkapuram et al. [27,28] assessed the thermal behaviour of pine needle fibre–reinforced PP composites. They observed a decrease in the degree of crystallinity with increased fibre content. The degree of crystallinity of PP and composite pellets had implications for their mechanical, thermal, and electrical properties [29]. In our study, both natural fibre samples exhibited a peak at 249–250°C, signifying the initiation of thermal degradation in main components, such as cellulose, hemicellulose, and lignin, as evidenced in the TGA analysis. The calculated enthalpy values around this peak were 63 J/g for flax fibre and 41 J/g for pine fibre. The enthalpy of this peak is directly proportional to the type and chemical composition of the natural fibres. The chemical composition of natural fibres varies based on factors including fibre type, plant part, processing, and aging. The chemical composition of flax fibre was primarily dominated by cellulose (68.7–75.5%), followed by hemicellulose (12.2–14%) and lignin (2.1–4.7%). In contrast, the chemical composition of pine fibre comprised 42% cellulose, 29% hemicellulose, and 28% lignin [8,13]. The peak observed at 460–464°C corresponded to the thermal degradation of PP. The calculated enthalpy values at this peak were 662 J/g for PP, 560 J/g for PP-flax, and 427 J/g for PP-pine.

The TGA results confirmed the four heat flow peaks identified in the DSC analysis. These peaks align with the four stages of thermal degradation observed in the samples: water evaporation, PP melting, the degradation of the main components of natural fibres, and PP degradation. The PP melting phenomenon is more distinctly evident in the DSC analysis. Both TGA and DSC outcomes provide insights into the thermal properties of flax fibres, pine fibres, and composite materials, encompassing parameters such as water content, crystallinity degree, thermal stability, melting temperature, and decomposition temperature.

Preprints.org (www.preprints.org) | NOT PEER-REVIEWED | Posted: 20 March 2024 doi:10.20944/preprints202403.1242.v1



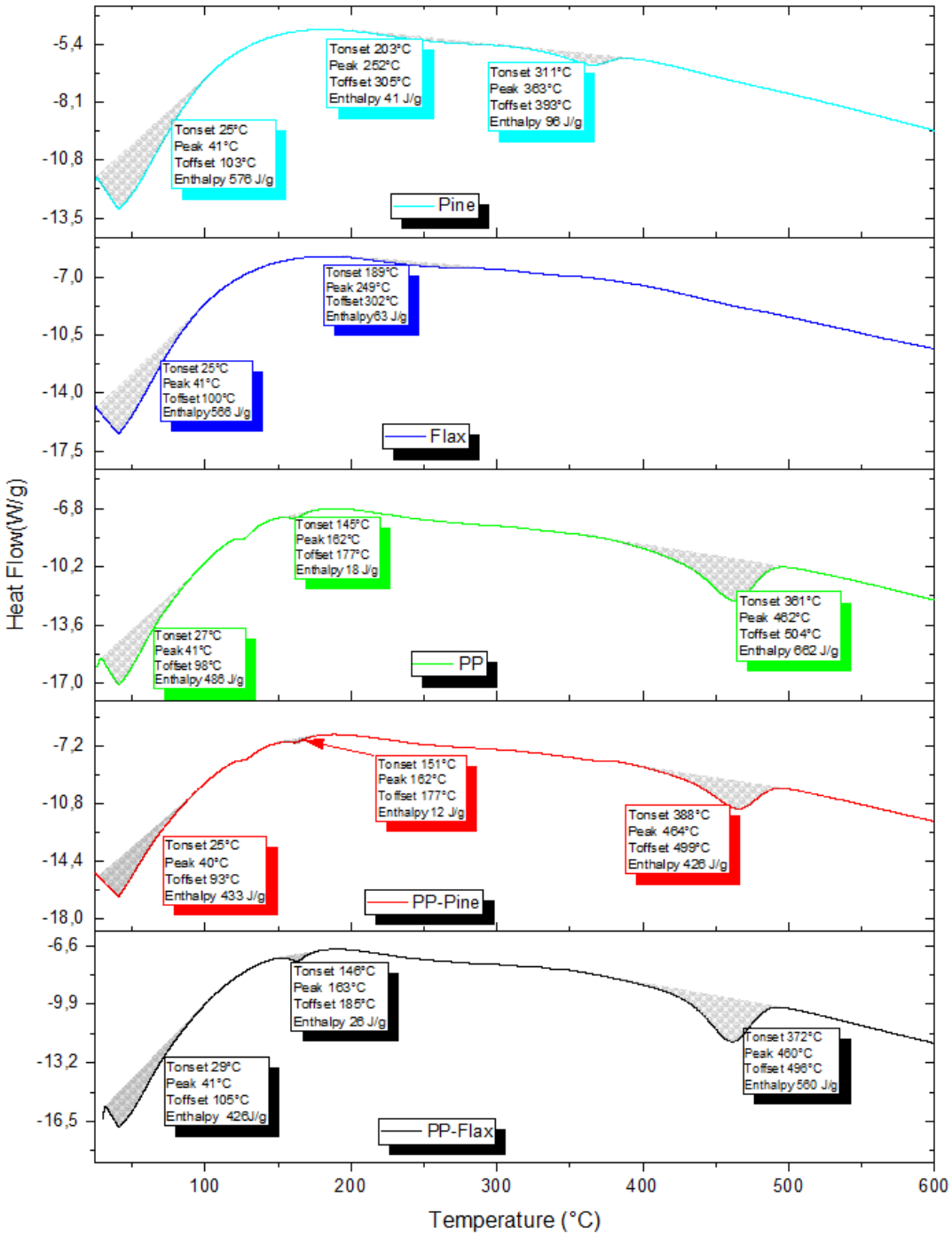


**Figure 5.** DSC curves for composite pellets and their constituents.

**Table 1.** DSC curves for composite pellets and their constituents.

| Materials | Temperature (°C) | | | Type of peak | Enthalpy (AH) (J/g) | Reference |
|---|---|---|---|---|---|---|
| | Onset | Peak | Offset | | | |
| *Atriplex halimus* ($NaHCO_3$) | 25.9 | 46.9 | 98.9 | Endothermic | 24.89 | [19] |
| | 277.9 | 321.9 | 357.9 | Exothermic | 155.05 | |
| *Atriplex halimus* (NaOH) | 20.1 | 42.1 | 95.1 | Endothermic | 29.10 | |
| | 296.1 | 335.1 | 381.1 | Exothermic | 74.73 | |
| | 438.1 | 464.1 | 498.1 | Exothermic | 42.21 | |
| *Flax* | 25.2 | 41.2 | 100.5 | Endothermic | 566.16 | Current work |
| | 189.9 | 249.1 | 302.3 | Endothermic | 63.74 | |

 doi:10.20944/preprints202403.1242.v1



| | | | | | |
|---|---|---|---|---|---|
| *Pine* | 25.6 | 41.5 | 103.3 | Endothermic | 576.6 |
| | 203.2 | 252.9 | 305.3 | Endothermic | 41.47 |
| | 311.2 | 363.4 | 393.2 | Endothermic | 96.84 |
| *PP* | 27.9 | 41.1 | 98.00 | Endothermic | 486.76 |
| | 112.7 | 127.0 | 137.97 | Endothermic | 16.68 |
| | 145.9 | 162.0 | 177.97 | Endothermic | 18.34 |
| | 361.7 | 462.1 | 504.05 | Endothermic | 662.12 |
| *PP-flax* | 29.9 | 41.8 | 105.5 | Endothermic | 426.93 |
| | 146.4 | 163.8 | 185.5 | Endothermic | 26.22 |
| | 372.1 | 460.8 | 496.6 | Endothermic | 560.47 |
| *PP-pine* | 25.40 | 40.96 | 93.36 | Endothermic | 433.73 |
| | 117.9 | 128.3 | 140.9 | Endothermic | 12.81 |
| | 151.2 | 162.6 | 177.4 | Endothermic | 12.10 |
| | 388.6 | 464.0 | 499.4 | Endothermic | 426.94 |

### *3.6. ATR–FTIR Analysis*

The ATR–FTIR test curves of Figure 6 show the absorption bands characteristic of the different functional groups in the five samples (PP, PP-pine, PP-flax, pine fibres, and flax fibres). The absorption bands are proportional to the concentration of the functional groups in the samples. The flax and pine fibres show similar absorption bands, corresponding to the functional groups of cellulose, hemicellulose, and lignin, the main components of natural fibres. The most critical absorption bands are those at 3340 $cm^{-1}$ (H–O stretching vibrations), 2920 $cm^{-1}$ (C–H stretching vibrations), 1734 $cm^{-1}$ (C=O stretching vibrations), 1593 $cm^{-1}$ (C=C aromatic stretched), 1234 $cm^{-1}$ (acetyl group C–O bond stretching vibrations), 1107 $cm^{-1}$ (C–O stretching vibrations of the ester group), 1049 $cm^{-1}$ (C–O–C stretched), and 796 $cm^{-1}$ (C–H deformed) [19,30,31].

The pine fibre shows a higher intensity of the absorption bands at 1734 $cm^{-1}$ and 1234 $cm^{-1}$ than the flax fibre, indicating a higher hemicellulose and lignin content in the pine fibre. Hemicellulose and lignin are the most amorphous components, and lignin is the most thermally stable component of natural fibres. The PP and the composites reinforced with flax and pine fibres show similar absorption bands, corresponding to the functional groups of PP, which is the polymer matrix of the composites. The most significant absorption bands are those at 2949 $cm^{-1}$ ($CH_3$ asymmetric stretching), 2916 $cm^{-1}$ (symmetric stretching of $CH_2$ ), 2848 $cm^{-1}$ ($CH_2$ asymmetric stretching), 1462 $cm^{-1}$ ($CH_3$ symmetrical bending), 1375 $cm^{-1}$ (CH3 symmetric deformation vibration), 1166 $cm^{-1}$ (C–H rocking), 997 $cm^{-1}$ ($CH_3$ asymmetric rocking vibration), 972 $cm^{-1}$ (e CH3 asymmetric rocking and the CC asymmetric stretching vibrations), 840 $cm^{-1}$ ($CH_3$ Rocking), and 719 $cm^{-1}$ (C–C stretching) [32–34].

The PP shows a higher intensity of the absorption bands at 2949 $cm^{-1}$, 2916 $cm^{-1}$, 2848 $cm^{-1}$, 1462 $cm^{-1}$, 1375 $cm^{-1}$, 1166 $cm^{-1}$, 997 $cm^{-1}$, 972 $cm^{-1}$, 840 $cm^{-1}$, and 719 $cm^{-1}$ than the composites reinforced with flax and pine fibres, indicating a higher content of PP compared to composite pellets. PP is the most thermoplastic and fusible component of the composites. Additionally, the peaks observed in the curves of the pine and flax fibres do not appear in the case of PP, PP-pine, and PP-flax. Therefore, a good coverage of the flax and pine fibre by the PP matrix is present. The same observation was recorded by Alam et al. [35].

### *3.7. Acoustic Emission Analysis*

Figures 6 and 7 illustrate the localization and distribution of AE signals or "hits" recorded during the test based on three parameters: burst amplitude, counts, and duration. The results are presented for non-aged specimens (Figure 6a and Figure 7a), specimens aged under dry conditions (Figure 6b and Figure 7b), and specimens aged under humidity (Figure 6c and Figure 7c) concerning the PP30-F and PP30-P samples, respectively. The amplitude range of AE signals associated with matrix cracking, matrix–matrix friction, decohesion, and fibre–matrix friction varies from 40 to 50 dB, 50 to

 doi:10.20944/preprints202403.1242.v1



60 dB, 55 to 75 dB, and 60 dB and above, respectively. Additionally, we observe that AE events are concentrated in the areas where the tested specimens have ruptured.

Results indicate that both materials exhibit similar damage mechanisms, including matrix cracking, matrix–matrix friction, decohesion, and fibre–matrix friction. However, the percentages of these mechanisms vary between the two materials. Prior to aging, PP30-F showed lower levels of decohesion compared to PP30-P at 12% and 21%, respectively. The predominant mechanism in both materials is matrix cracking, accounting for 56% in PP30-F and 64% in PP30-P. After aging, a significant increase in the percentage of matrix cracking was observed in both materials, possibly due to the formation of microcracks under UV exposure. These superficial microcracks, which were generated at the PP matrix level, propagated during tensile tests, leading to an increase in the percentage of matrix cracking after aging. The figures 6(a), 6(b), and 6(c) reveal an 18% and 19% increase in matrix cracking for Conditions 1 and 2 for PP30-F, while PP30-P shows increases of 11% and 14%, respectively.

When both materials were exposed to UV rays or high temperatures, photo-oxidation reactions occurred in the lignin of natural fibres, and moisture accelerated these reactions. The velocity of photo-oxidation reactions in biocomposites depends on the chemical composition of the natural fibres. The high level of lignin present in pine fibres can act as a UV absorber, mitigating the damage and degradation of the HDPE-pine composite compared to flax fibres. Additionally, the matrix cracking of outdoor biocomposite structures deteriorates significantly more in a humid environment than in a dry one due to increased chemical reactivity [6,9,11]. The tests were conducted three times, and the results demonstrated high precision, with minimal standard deviations in all measurements, ensuring the reliability of the obtained data. These observations highlight the impact of UV aging on the damage mechanisms of biocomposites and underscore the importance of understanding these phenomena for the development of durable and resilient materials for various industrial applications.

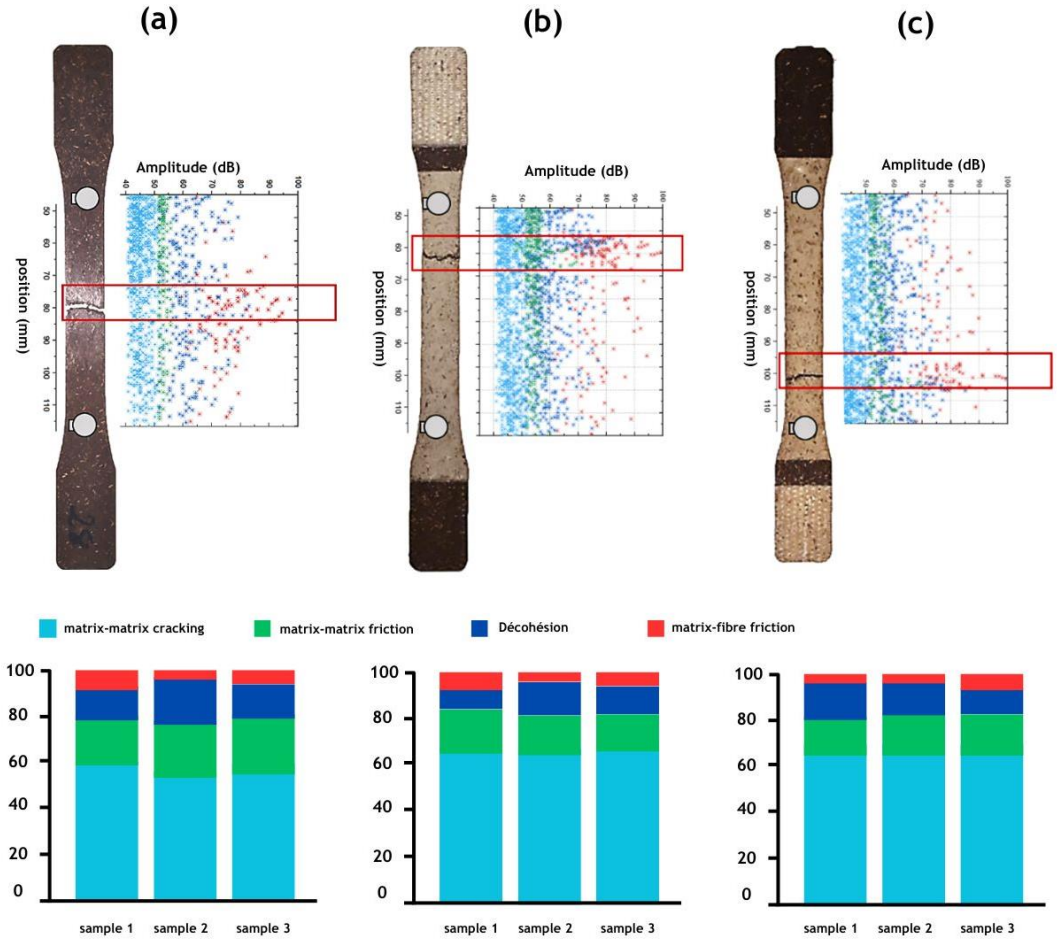

 doi:10.20944/preprints202403.1242.v1



**Figure 6.** Amplitude versus location of acoustic events recorded during a tensile test on the PP30-F sample for (a) the non-aged condition, (b) Condition 1, and (c) Condition 2 compared with the sample picture after failure.

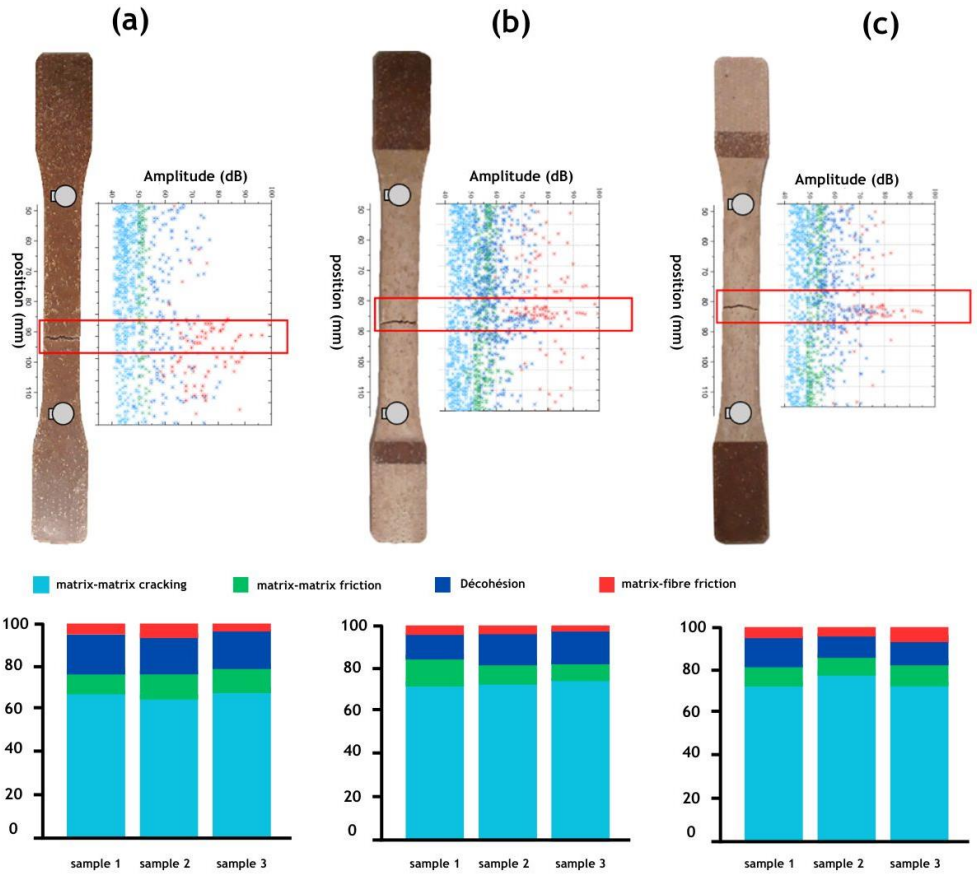


**Figure 7.** Amplitude versus location of acoustic events recorded during a tensile test on PP30-P sample for (a) the non-aged condition, (b) Condition 1 and (c) Condition 2 in comparison with the sample picture after failure.

## 4. Conclusions

This study provides a comprehensive overview of the effect of the chemical composition of plant fibres on the UV aging behaviour of biocomposites reinforced with flax and pine fibres. Following the detailed analysis of PP-flax and PP-pine fibre composites and their components, several significant conclusions can be drawn. First, the chemical composition of plant fibres, particularly the lignin content, directly impacts the durability of composites against UV effects. By precisely identifying the composition of the granules, we could better understand the thermal behaviour and potential damage mechanisms, which are crucial for the development of resistant materials.

Microscopic images of the fibres revealed distinct characteristics, such as *L*/*D* and density, with different values for flax and pine. These differences are also reflected in the thermal properties of the composites, wherein the lignin content of pine fibres delays thermal degradation compared to flax fibres.

TG and DSC analysis confirmed the complexity of the thermal degradation processes of the composites, highlighting the different stages of decomposition of the individual constituents. Additionally, ATR–FTIR spectra identified functional groups present in natural fibres and PP, thus strengthening the understanding of the interaction between phases of the composite.

Lastly, the results of the AE tests revealed similar damage mechanisms between the two composites, highlighting their sensitivity to UV-induced microcracks. These findings underscore the importance of continuing research into the development of composites resistant to environmental

 doi:10.20944/preprints202403.1242.v1



conditions, considering the specific properties of natural fibres and their interaction with the polymer matrix.

## References


1. Jaiswal, C. *Biocomposites Market Research Report Information*; February 2024; p 140 pages.
2. Ramesh, M.; Rajeshkumar, L.; Sasikala, G.; Balaji, D.; Saravanakumar, A.; Bhuvaneswari, V.; Bhoopathi, R., A critical review on wood-based polymer composites: Processing, properties, and prospects. *Polymers* **2022,** 14, (3), 589.
3. Beg, M. D. H.; Pickering, K. L., Accelerated weathering of unbleached and bleached Kraft wood fibre reinforced polypropylene composites. *Polymer Degradation and Stability* **2008,** 93, (10), 1939-1946.
4. Fabiyi, J. S.; McDonald, A. G.; Wolcott, M. P.; Griffiths, P. R., Wood plastic composites weathering: Visual appearance and chemical changes. *Polymer degradation and stability* **2008,** 93, (8), 1405-1414.
5. Belec, L.; Nguyen, T.; Nguyen, D.; Chailan, J.-F., Comparative effects of humid tropical weathering and artificial ageing on a model composite properties from nano-to macro-scale. *Composites Part A: Applied Science and Manufacturing* **2015,** 68, 235-241.
6. Peng, Y.; Liu, R.; Cao, J., Characterization of surface chemistry and crystallization behavior of polypropylene composites reinforced with wood flour, cellulose, and lignin during accelerated weathering. *Applied Surface Science* **2015,** 332, 253-259.
7. Chang, B. P.; Mohanty, A. K.; Misra, M., Studies on durability of sustainable biobased composites: a review. *RSC advances* **2020,** 10, (31), 17955-17999.
8. Nasri, K.; Toubal, L.; Loranger, É.; Koffi, D., Influence of UV irradiation on mechanical properties and drop-weight impact performance of polypropylene biocomposites reinforced with short flax and pine fibers. *Composites Part C: Open Access* **2022,** 9, 100296.
9. Nasri, K.; Toubal, L., Experimental and numerical investigation of damage and mechanical property retention by bio-composite plastic made with flax or pinewood fiber and aged by exposure to ultraviolet light. *Journal of Building Engineering* **2023,** 79, 107899.
10. Dittenber, D. B.; GangaRao, H. V., Critical review of recent publications on use of natural composites in infrastructure. *Composites Part A: applied science and manufacturing* **2012,** 43, (8), 1419-1429.
11. Azwa, Z.; Yousif, B.; Manalo, A.; Karunasena, W., A review on the degradability of polymeric composites based on natural fibres. *Materials & Design* **2013,** 47, 424-442.
12. Morin, S.; Dumoulin, L.; Delahaye, L.; Jacquet, N.; Richel, A., Green composites based on thermoplastic starches and various natural plant fibers: Impacting parameters of the mechanical properties using machine-learning. *Polymer Composites* **2021,** 42, (7), 3458-3467.
13. Nasri, K.; Loranger, É.; Toubal, L., Effect of cellulose and lignin content on the mechanical properties and drop-weight impact damage of injection-molded polypropylene-flax and-pine fiber composites. *Journal of Composite Materials* **2023**, 00219983231186208.
14. Matuana, L. M.; Jin, S.; Stark, N. M., Ultraviolet weathering of HDPE/wood-flour composites coextruded with a clear HDPE cap layer. *Polymer degradation and stability* **2011,** 96, (1), 97-106.
15. Bravo, A.; Toubal, L.; Koffi, D.; Erchiqui, F., Damage characterization of bio and green polyethylene–birch composites under creep and cyclic testing with multivariable acoustic emissions. *Materials* **2015,** 8, (11), 7322-7341.
16. International, A., *Standard test method for tensile properties of plastics*. ASTM international: 2014.
17. ASTM, G., 53. Practice for operating light-and water-exposure apparatus (fluorescent UV-condensation type) for exposure of nonmetallic materials. *Annual Book of ASTM Standards* **1996,** 14.
18. Vinod, A.; Rangappa, S. M.; Srisuk, R.; Tengsuthiwat, J.; Siengchin, S., Agro-waste Capsicum annum stem: An alternative raw material for lightweight composites. *Industrial Crops and Products* **2023,** 193, 116141.
19. Belouadah, Z.; Belhaneche-Bensemra, N.; Ati, A., Characterization of ligno-cellulosic fiber extracted from Atriplex halimus L. plant. *International Journal of Biological Macromolecules* **2021,** 168, 806-815.
20. Burhenne, L.; Messmer, J.; Aicher, T.; Laborie, M.-P., The effect of the biomass components lignin, cellulose and hemicellulose on TGA and fixed bed pyrolysis. *Journal of Analytical and Applied Pyrolysis* **2013,** 101, 177-184.
21. Kristanto, J.; Azis, M. M.; Purwono, S., Multi-distribution activation energy model on slow pyrolysis of cellulose and lignin in TGA/DSC. *Heliyon* **2021,** 7, (7).
22. Yi, Y.; Wang, X.; Liu, Z.; Gao, C.; Fatehi, P.; Wang, S.; Kong, F., A green composite hydrogel based on xylan and lignin with adjustable mechanical properties, high swelling, excellent UV shielding, and antioxidation properties. *Journal of Applied Polymer Science* **2022,** 139, (28), e52520.
23. Sonawane, S.; Thakur, P.; Paul, R., Study on thermal property enhancement of MWCNT based polypropylene (PP) nanocomposites. *Materials Today: Proceedings* **2020,** 27, 550-555.

 doi:10.20944/preprints202403.1242.v1




24. Sun, H.; Zhao, Z.; Yang, Q.; Yang, L.; Wu, P., The morphological evolution and β-crystal distribution of isotactic polypropylene with the assistance of a long chain branched structure at micro-injection molding condition. *Journal of Polymer Research* **2017,** 24, 1-13.
25. Bahrami, R.; Bagheri, R., Effect of hybridization on crystallization behavior, mechanical properties, and toughening mechanisms in rubber-modified polypropylene flax fiber composites. *Journal of Composite Materials* **2022,** 56, (17), 2677-2693.
26. Sergi, C.; Tirillò, J.; Iacovacci, C.; Sarasini, F., Influence of reprocessing cycles on the morphological, thermal and mechanical properties of flax/basalt hybrid polypropylene composites. *Sustainable Materials and Technologies* **2023**, e00648.
27. Ming-Zhu, P.; Chang-Tong, M.; Xu-Bing, Z.; Yun-Lei, P., Effects of rice straw fiber morphology and content on the mechanical and thermal properties of rice straw fiber-high density polyethylene composites. *Journal of Applied Polymer Science* **2011,** 121, (5), 2900-2907.
28. Malkapuram, R.; Kumar, V.; Negi, Y. S., Novel treated pine needle fiber reinforced polypropylene composites and their characterization. *Journal of reinforced plastics and composites* **2010,** 29, (15), 2343-2355.
29. Sullivan, E. M.; Oh, Y. J.; Gerhardt, R. A.; Wang, B.; Kalaitzidou, K., Understanding the effect of polymer crystallinity on the electrical conductivity of exfoliated graphite nanoplatelet/polylactic acid composite films. *Journal of Polymer Research* **2014,** 21, 1-9.
30. Odalanowska, M.; Skrzypczak, A.; Borysiak, S., Innovative ionic liquids as functional agent for wood-polymer composites. *Cellulose* **2021,** 28, 10589-10608.
31. Siva, R.; Valarmathi, T.; Palanikumar, K., Effects of magnesium carbonate concentration and lignin presence on properties of natural cellulosic Cissus quadrangularis fiber composites. *International Journal of Biological Macromolecules* **2020,** 164, 3611-3620.
32. Jeyavani, J.; Sibiya, A.; Gopi, N.; Mahboob, S.; Riaz, M. N.; Vaseeharan, B., Dietary consumption of polypropylene microplastics alter the biochemical parameters and histological response in freshwater benthic mollusc Pomacea paludosa. *Environmental Research* **2022,** 212, 113370.
33. Mansuroglu, D.; Mecit, G.; Uzun-Kaymak, I. U., A study of crystallization in plasma modified polypropylene. *Materials Today: Proceedings* **2019,** 18, 1964-1971.
34. Chinnadurai, T.; Arungalai Vendan, S.; Rusu, C.; Scutelnicu, E., Experimental investigations on the polypropylene behavior during ultrasonic welding. *Materials and Manufacturing Processes* **2018,** 33, (7), 718-726.
35. Alam, L.; Piezel, B.; Sicot, O.; Aivazzadeh, S.; Moscardelli, S.; Van-Schoors, L., UV accelerated aging of unidirectional flax composites: Comparative study between recycled and virgin polypropylene matrix. *Polymer Degradation and Stability* **2023,** 208, 110268.